



# Synthesis and Characterization of a new hybrid material (MOF-5/Mag-H<sup>+</sup>) based on a Metal-Organic Framework and a Proton Exchanged Montmorillonite Clay (Maghnite-H<sup>+</sup>) as catalytic support

S. Bennabi\*, M. Belbachir

Laboratory of Polymer Chemistry, Department of Chemistry, Faculty of Exact and Applied Sciences, University of Oran I  
Ahmed BenBella, BP 1524 El M'Naouar, 31000 Oran, Algeria

Received 24 Mar 2016,  
Revised 17 Sep 2016,  
Accepted 26 Sep 2016

## Keywords

- ✓ MOF-5;
- ✓ Maghnite-H<sup>+</sup>;
- ✓ catalytic support;
- ✓ in-situ polymerization
- ✓ MAS NMR studies;
- ✓ Thermal properties

[souad\\_bennabi02@yahoo.fr](mailto:souad_bennabi02@yahoo.fr)

Phone: +213 776 289 166

Fax: +213 415 81413

## Abstract

Metal-organic framework MOF-5 is a microporous material with a large specific surface area and high porosity. It is mainly used in the field of automobile industry as a container for storing hydrogen (alternative fuel) and for a prevention of the environment by trapping CO<sub>2</sub> (greenhouse gas emissions). The present study shows the synthesis of this material using a clay called Maghnite-H<sup>+</sup> as catalytic support with the aim to respect the principles of green chemistry, in order to enhance the yield which increases from 35% to 63% and improve the thermal stability with a gain of 40°C for MOF-5/Mag-H<sup>+</sup>. The structure of this hybrid material is established by <sup>13</sup>C MAS NMR and confirmed by FT-IR. <sup>27</sup>Al MAS NMR and <sup>29</sup>Si MAS NMR results show that there are interactions between the chains of MOF-5 and the silicate surface or aluminum of Maghnite-H<sup>+</sup>. Moreover, X-Ray Fluorescence confirms that Maghnite-H<sup>+</sup> used in the synthesis of MOF-5, at different weight percentages, keeps the same elemental and chemical composition. X-Ray Diffraction reveals the formation of a partially exfoliated/partially intercalated structure.

## 1. Introduction

In the last decade, porous coordination polymers (PCP) with infinite structures have been intensively studied. These compounds are MOFs : Metal-Organic Frameworks. Their syntheses are based on the use of a vast variety of metal ions (clusters), i.e. inorganic nodal points, interconnected by organic ligands to form rigid and oriented Metal-Oxygen-carbon (M-O-C) groups [1]. MOFs offer potential applications in catalysis, ion exchange, separation and polymerization due to their extremely large surface area, diverse means available for functionalization and well-ordered porous structures with a various geometry : one-dimensional 1D (channels), two-dimensional 2D (layers) and three-dimensional 3D (networks) [2]. MOFs have also attracted considerable attention in the field of adsorption as a means of storage of fuel gases, such as hydrogen and methane in order to promote utilization of adsorbed natural gas (ANG), as well as trapping CO<sub>2</sub> which is a greenhouse gas [3-5].

Several methods of synthesis of MOFs have been reported in the literature such as ultrasonic enhanced [6], microwave heated [7], diffusion or direct addition of amines [8] and growth on substrates [9]. Nevertheless, solvothermal synthesis is the most commonly applied synthetic route leading to fast growth of crystals with high levels of crystallinity, phase purity and surface areas [10]. While synthetic techniques, such as mechanochemical synthesis, can reduce solvent usage significantly when producing MOFs with high yields [11]. However, for an industrially viable product to be formed, bridging the gap to scalable continuous processing is essential. Therefore, crystals of MOFs can be formed in a scalable solvothermal continuous process with a maximum space time yield of nearly 1000 kg.m<sup>-3</sup>.day<sup>-1</sup> [12].

One of the most representative MOFs is MOF-5 [Zn<sub>4</sub>O(BDC)<sub>3</sub>, BDC]. It is a structure which is formed by groups of (Zn<sub>4</sub>O)<sub>6</sub><sup>+</sup> and extended in a 3D network with BDC (1,4-benzenedicarboxylic acid) to produce a simple cubic lattice, with BET surface area from 260 m<sup>2</sup>/g to 4400 m<sup>2</sup>/g and with good thermal stability up to 400°C [13]. The amount of methane absorbed in different zeolites is proportional to their specific surface areas, therefore, MOF-5 is a transporter of fuel more convenient due to the properties of its cavities that easily adapt by creating linkages (Van Der Waals forces, hydrogen bonds) [14].

In this work, we propose a new approach for the synthesis of MOF-5. It consists in the use of a clay called Maghnite-H<sup>+</sup>. It is natural, more efficient, less expensive and less polluting to the environment with the aim to respect the principles of green chemistry [15]. It has a lamellar structure and shows remarkable catalytic capacities towards various polymerization reactions. Maghnite-H<sup>+</sup> is going to play the role of a

catalytic support to improve the yield of MOF-5 obtained but especially to increase its temperature stability which is crucial.

## 2. Experimental

### 2.1. Materials

The Maghnite used in this work comes from a quarry located in Maghnia (North West of Algeria) and was supplied by company “ENOF” (Algerian manufacture specialized in the production of nonferrous products and useful substances). Terephthalic acid (BDC: 1,4-benzenedicarboxylic acid) (Aldrich, 98%), Zinc nitrate Hexahydrate [ $\text{Zn}(\text{NO}_3)_2 \cdot 6\text{H}_2\text{O}$ ] (Aldrich, 98%) and N,N-Dimethylformamide (DMF) (Aldrich, 99.8%) were used as received without further purification.

### 2.2. Preparation of Maghnite- $\text{H}^+$

The preparation of Maghnite- $\text{H}^+$  is carried out by using a method similar to that described by Belbachir and co-workers [16]. In an Erlenmeyer flask of 500 ml, 30 g of crushed and dried raw-maghnite are dispersed in 120 ml of distilled water, the mixture is stirred for 2 hours. After this time, 100 ml of 2.5M sulfuric acid solution is added, the solution thus obtained is kept under stirring for two days at room temperature. Then, the product is filtered and washed with distilled water until complete disappearance of traces of acid. Once purified clay, it is dried overnight in an oven at  $105^\circ\text{C}$ , and then stored in vials well sealed against moisture and any impurity.

### 2.3. Synthesis of MOF-5

MOF-5 is prepared according to the method of Yaghi and co-workers [17]. A typical synthesis of MOF-5 is performed by using an established solvothermal synthesis, employing DMF as the solvent. Zinc nitrate hexahydrate (3.0 g, 11 mmol) and 1,4-benzenedicarboxylic acid (0.75 g, 4.5 mmol) are dissolved in 100 ml of DMF. The solution is kept in a closed vessel and white crystals are observed after heating the reaction mixture at  $100^\circ\text{C}$  for 18h. During filtration, the crystals are washed several times with fresh solvent. The solid is stored under dry DMF. The yield is 35.17%. Figure 1 summarizes the synthesis conditions:

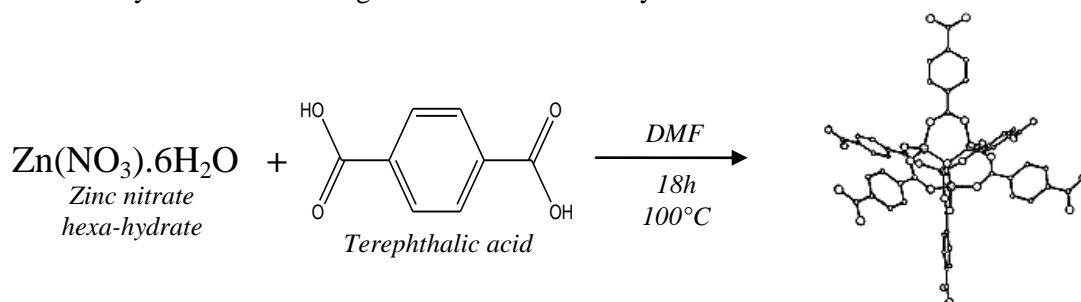


Figure 1: Synthesis reaction of MOF-5

MOF-5

### 2.4. Synthesis of MOF-5 with Maghnite- $\text{H}^+$

MOF-5/Mag- $\text{H}^+$  is synthesized by in-situ polymerization of zinc nitrate and 1,4-benzenedicarboxylic acid (BDC) with an amount of Maghnite- $\text{H}^+$  in DMF. The mixture is kept in thermostat ( $100^\circ\text{C}$ ) for 18 hours. The product is collected by filtration and washed several times with fresh solvent and stored under dry DMF. Figure 2 summarizes the synthesis conditions:

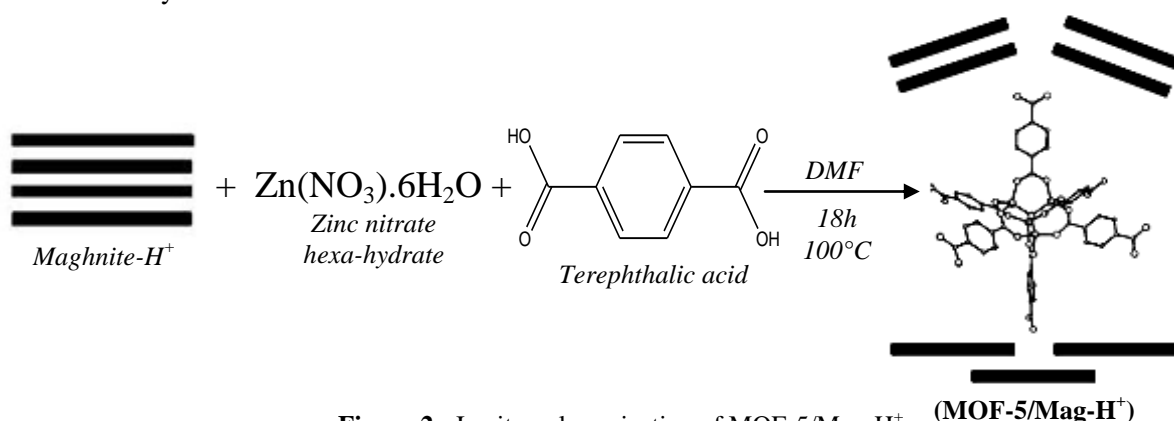


Figure 2: In-situ polymerization of MOF-5/Mag- $\text{H}^+$

(MOF-5/Mag- $\text{H}^+$ )

#### 2.4.1. Effect of the amount of Maghnite-H<sup>+</sup> on the polymerization of MOF-5

Table 1 shows the effect of the amount of Maghnite-H<sup>+</sup> on the polymerization yield. Indeed, the yield increases with the increase in the amount of Maghnite-H<sup>+</sup>. This is mainly due to the number of active sites in the catalyst responsible for the initiation of the polymerization reaction until a maximum amount of the catalyst (25%wt of Maghnite-H<sup>+</sup>) from which the yield remains unchanged, in this case, the catalyst acts as a co-monomer participating in the reaction.

**Table 1:** Effect of the amount of Maghnite-H<sup>+</sup> on the polymerization of MOF-5.

Maghnite-H <sup>+</sup> (% by weight)	Yield (%) of MOF-5/Mag-H <sup>+</sup>
5	42.13
10	54.76
25	63.03
40	63.65
50	63.20
60	63.34

#### 2.5. Characterizations

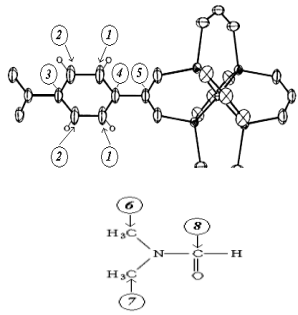
Solid State <sup>13</sup>C, <sup>27</sup>Al and <sup>29</sup>Si MAS NMR spectra (MAS NMR: Magic Angle Spinning Nuclear Magnetic Resonance) are recorded with a Bruker spectrometer (Avance III 400WB). The sample spinning frequency is 10 kHz for <sup>13</sup>C, 5 kHz for <sup>29</sup>Si and 12 kHz for <sup>27</sup>Al. FT-IR (Fourier Transform Infrared spectroscopy) absorption spectra are recorded on an MATTSON GENESIS II FT-IR spectrometer using the KBr pressed disc technique. X-ray fluorescence (XFR) analysis is carried out using the AXIOS-4kW sequential XRF-spectrometer with sample changer. Powder X-ray diffraction (DRX) patterns are collected on an AXIOS spectrometer in transmission mode in the form of powder supported between two foils, which are then clamped in the PW1818/40 sample holder for as-prepared samples, the foil used is Mylar 3.6 microns. Thermogravimetric analyzes (ATG) are recorded on a SETARAM Labsys TG-DTA/DSC (room temperature - 1600°C) with a nitrogen sweep of 200 mL/min. The temperature ramp is 10°C/min.

### 3. Results and discussion

#### 3.1. Structure determination of MOF-5/Mag-H<sup>+</sup>

The different signals observed in the spectra of <sup>13</sup>C MAS NMR (Figure 3) and which are summarized in Table 2, correspond to the groups shown in the structural formulas of MOF-5 and MOF-5/Mag-H<sup>+</sup> containing 01%, 25% and 50% by weight of Maghnite-H<sup>+</sup>. These spectra confirm the disappearance of the peak corresponding to carboxylic function (COOH) at 182 ppm and the appearance of the peak at 172 ppm which is attributed to ester function (COO). The spectra show also the peaks corresponding to DMF trapped in MOF-5 and MOF-5/Mag-H<sup>+</sup>. <sup>13</sup>C MAS NMR spectra of MOF-5 and for MOF-5/Mag-H<sup>+</sup> are nearly identical. In fact, the chemical shifts of different groups confirm the structure of these products. The spectra show particularly that the structure of MOF-5 is not altered by the addition of Maghnite-H<sup>+</sup>.

**Table 2:** Different signals of Carbons of MOF-5, MOF-5/Mag-H<sup>+</sup> and DMF.

(1) 128 ppm (2) 130 ppm (3) 136 ppm (4) 137 ppm (5) 172 ppm (6) 35 ppm (7) 30 ppm (8) 162 ppm	
--	---

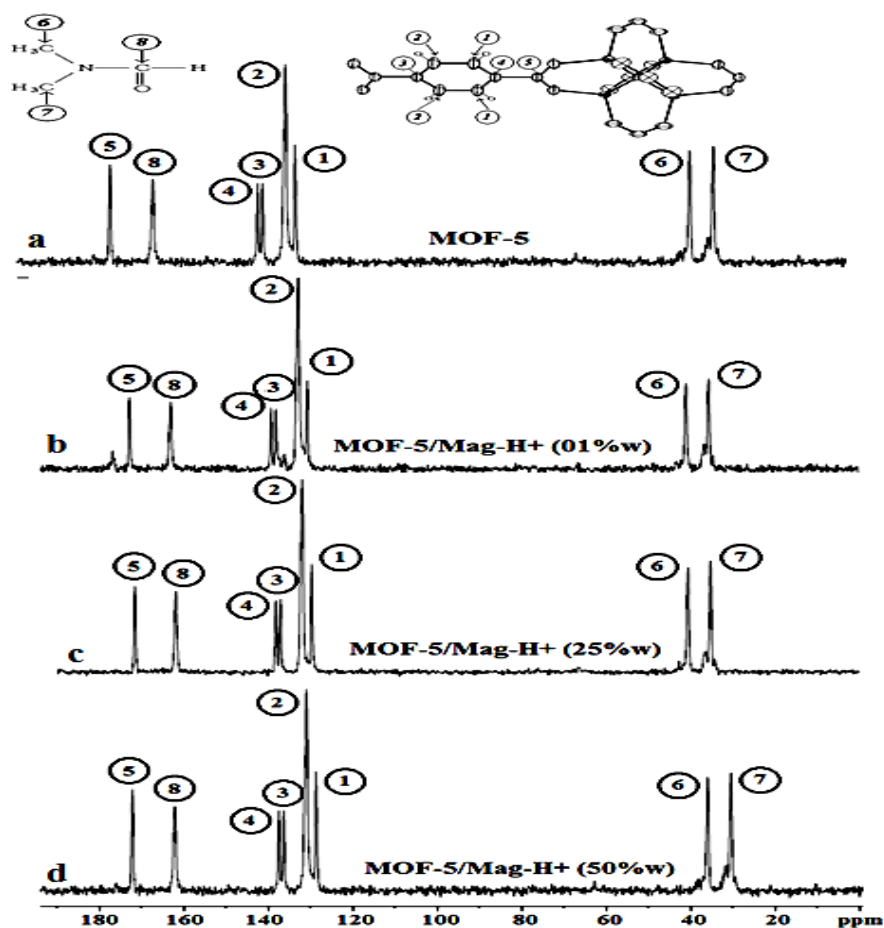


**Figure 3:**  $^{13}\text{C}$  MAS NMR spectra of: a) MOF-5, b) MOF-5/Mag-H $^+$  (1%w), c) MOF-5/Mag-H $^+$  (25%w), d) MOF-5/Mag-H $^+$  (50%w) and DMF.

The ability of  $^{27}\text{Al}$  MAS NMR to distinguish between  $\text{AlO}_4$  and  $\text{AlO}_6$  units is very informative for structural characterization. Because  $^{27}\text{Al}$  nucleus has a very high natural sensitivity and reasonably short relaxation time, NMR spectra with good signal to noise ratio can be obtained easily [18]. The  $^{27}\text{Al}$  MAS spectra (Figure 4) provides information about the local environment of the aluminum sites in Maghnite-H $^+$  and MOF-5/Mag-H $^+$ .

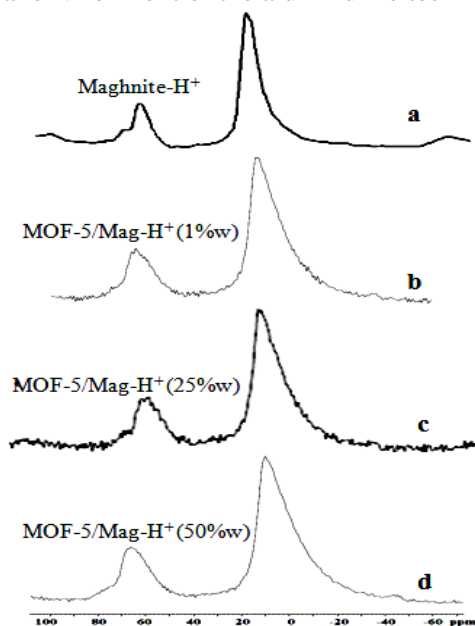


**Figure 4:**  $^{27}\text{Al}$  MAS NMR spectra of: a) MOF-5, b) MOF-5/Mag-H $^+$  (1%w), c) MOF-5/Mag-H $^+$  (25%w) and d) MOF-5/Mag-H $^+$  (50%w)

Figure 5 shows the  $^{29}\text{Si}$  MAS NMR spectra of Maghnite- $\text{H}^+$  and MOF-5/Mag- $\text{H}^+$ . These spectra provide supporting evidence for no change occurring on silicate sites of the clay. In fact, in all spectra, there is resonance at -110 ppm which is assigned to the amorphous silica  $\text{SiO}_2$   $\text{Q}^4$  (OAl) [23,24]. The spectra of Maghnite- $\text{H}^+$  shows also an intense signal of Si  $\text{Q}^3$  (OAl) at -93 ppm corresponding to tetrahedral silicon  $\text{Si}^{4+}$  where each ion is surrounded by three silicon ions. However, the same signal is observed at -88 ppm for MOF-5/Mag- $\text{H}^+$  at different percentage by weight of Maghnite- $\text{H}^+$ . This small change of about 5 ppm observed between the  $^{29}\text{Si}$  MAS NMR spectra of Maghnite- $\text{H}^+$  and that of MOF-5/Mag- $\text{H}^+$  could be induced either by interactions of the polymer chains with the silicate surface or local environmental changes on neighboring aluminum sites upon grafting.

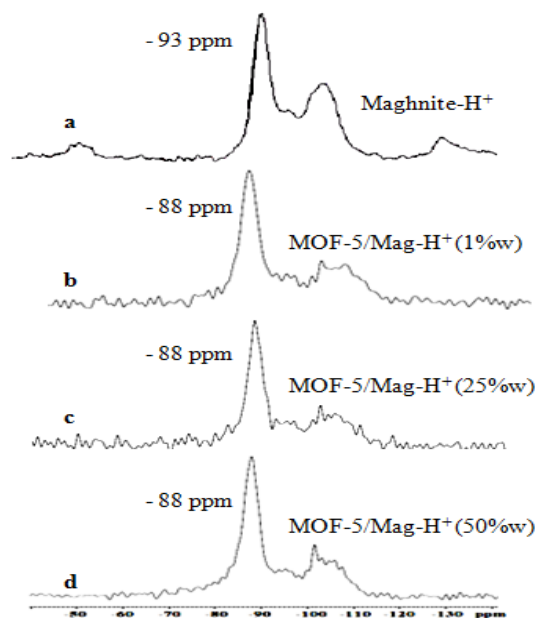


**Figure 5:**  $^{29}\text{Si}$  MAS NMR spectra of : a) MOF-5, b) MOF-5/Mag- $\text{H}^+$  (1%w), c) MOF-5/Mag- $\text{H}^+$  (25%w) and d) MOF-5/Mag- $\text{H}^+$  (50%w)

On all the spectra, two small bands can be distinguished at apparent chemical shifts of 58–60 ppm and 68–71 ppm and which are assigned to  $\text{AlO}_4$  octahedric sites in the Maghnite structure as a consequence of isomorphic ions substitution within the silicate layers. Another dominant asymmetric line at apparent chemical shifts of 3–4 ppm is assigned to  $\text{AlO}_6$  sites within the octahedral sheets of the clay [19–22]. All spectra are similar, indicating that the aluminosilicate layers of the clay are not chemically modified by their incorporation in MOF-5 during the polymerization process.

FT-IR measurements (Figure 6) are in a good agreement with MOF-5 and MOF-5/Mag- $\text{H}^+$  structures. Indeed, when comparing the different frequencies of characteristic groups, we find that there is disappearance of the intense and large characteristic band of O-H between 2500 and 3340  $\text{cm}^{-1}$  in FT-IR spectra of MOF-5 and MOF-5/Mag- $\text{H}^+$  confirming that there is a complete deprotonation of terephthalic acid and that the polymerization has occurred. These IR spectra also show the DMF solvent absorption frequencies characterized by vibration of C=O at 1656  $\text{cm}^{-1}$  and vibration of C-N at 1105  $\text{cm}^{-1}$ . In FT-IR spectra of MOF-5/Mag- $\text{H}^+$ , we find the usual characteristic frequencies of Maghnite- $\text{H}^+$ , in particular a broad band which represents the vibration of Si-O at 1039  $\text{cm}^{-1}$ , and a band of deformation Si-O-Si at 465  $\text{cm}^{-1}$ .

### 3.2. Morphology of the resulting MOF-5/Mag- $\text{H}^+$

Analysis by X-Ray Fluorescence (XRF) provides the different concentrations by weight into compounds of MOF-5 and MOF-5/Mag- $\text{H}^+$  as well as the ratio (Si/Al) which are calculated for each sample. The results summarized in Table 3 indicate that all MOF-5/Mag- $\text{H}^+$  contain: Si (main element), Al, and traces of K and Mg, same elements which constitute the elementary composition of Maghnite- $\text{H}^+$  alone. Also, the ratios (Si/Al) have nearly all the same value, showing that the Maghnite- $\text{H}^+$  used in the synthesis of MOF-5 keeps the same chemical composition in different percentages. In all obtained products, Zn contribution is clearly shown, since the zinc nitrate  $\text{Zn}(\text{NO}_3)_2$  is used for the preparation of all samples. Furthermore, it should be noted that the various weights of Maghnite- $\text{H}^+$  used in the synthesis of MOF-5 have a significant impact on the concentration of ZnO which decreases with the increase in the weight of Maghnite- $\text{H}^+$ , this is explained by the fact that its

crystalline structure is affected by the presence of other ions. Nevertheless, concentrations of ZnO in MOF-5 as well as in MOF-5/Mag-H<sup>+</sup> (25% wt) are almost identical, this result means that both structures are relatively the same and the ideal percentage by weight of Maghnite-H<sup>+</sup> is 25%.

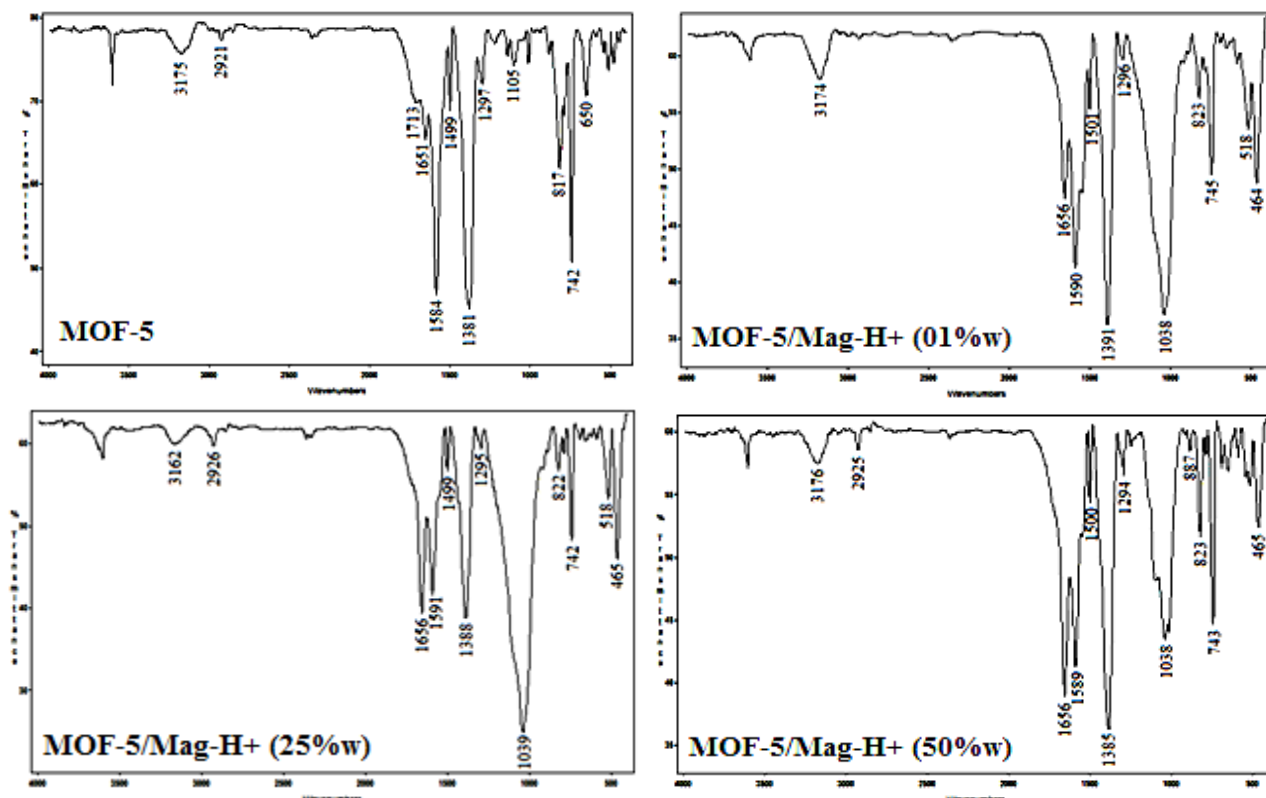


**Figure 6:** FT-IR spectra of MOF-5, MOF-5/Mag-H<sup>+</sup> containing 01%, 25% and 50% by weight of Maghnite-H<sup>+</sup> and DMF.

**Table 3:** Concentrations by weight into compounds of Maghnite-H<sup>+</sup>, MOF-5 and MOF-5/Mag-H<sup>+</sup> containing 1%, 25% and 50% by weight of Maghnite-H<sup>+</sup>.

	SiO <sub>2</sub>	Al <sub>2</sub> O <sub>3</sub>	MgO	K <sub>2</sub> O	ZnO	Si/Al
<i>MOF-5/Mag-H<sup>+</sup></i> (1% <sub>w</sub> )	14.614	4.274	0.953	0.291	79.869	3.41
<i>MOF-5/Mag-H<sup>+</sup></i> (25% <sub>w</sub> )	62.298	15.601	2.757	1.342	17.601	3.99
<i>MOF-5/Mag-H<sup>+</sup></i> (50% <sub>w</sub> )	70.453	17.331	2.814	1.679	5.981	4.06
<i>MOF-5</i>	-	-	-	-	17.820	-
<i>Maghnite-H<sup>+</sup></i>	57.54	14.45	2.58	0.46	-	3.98

The morphology of MOF-5 and MOF-5/Mag-H<sup>+</sup> (25% wt) (Figure 7) is studied by X-ray diffraction (XRD). First, the two compounds diffractometers showed that there is a great similarity between the overall profile of these materials, suggesting that these two compounds have the same structure phase and that the Maghnite-H<sup>+</sup> does not alter the final layout of MOF-5/Mag-H<sup>+</sup>. The intense peak below 10° (2θ = 9.8° corresponding to d = 9.1 Å) is observed in MOF-5 and MOF-5/Mag-H<sup>+</sup> diffractometers. This peak is the result of a distortion of the cubic symmetry in the structure of MOF-5 [25]. However, XRD pattern of MOF-5/Mag-H<sup>+</sup> shows also that there is a broad peak in the area of small angles (2θ = 6.7° corresponding to d = 13.3 Å) corresponding to the montmorillonite which is the main component of Maghnite-H<sup>+</sup>. This peak confirms the presence of the clay in the structure of MOF-5/Mag-H<sup>+</sup>. This result allows to conclude that there is formation of a partially exfoliated/partially intercalated structure. Indeed, the increase in the interlayer distance from 9,9 Å (Figure 8a) to 13,3 Å (Figure 8b) suggests intercalation of some chains of MOF-5 between the layers of clay. In the other hand, the exfoliated part of the structure is caused by the high molecular weight of MOF-5. This exfoliation is confirmed by FT-IR spectrum of MOF-5/Mag-H<sup>+</sup> (25% wt) which has a characteristic band at 465 cm<sup>-1</sup> attributed to the Si-O-Si.

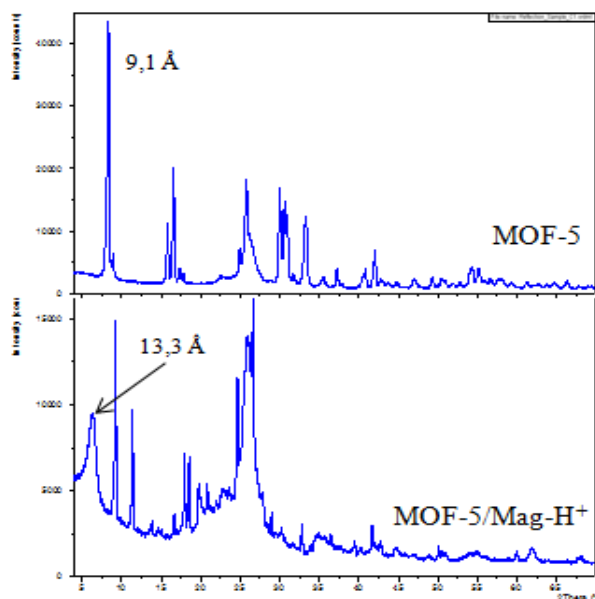


**Figure 7:** XRD patterns of MOF-5 and MOF-5/Mag-H<sup>+</sup> (25% w).

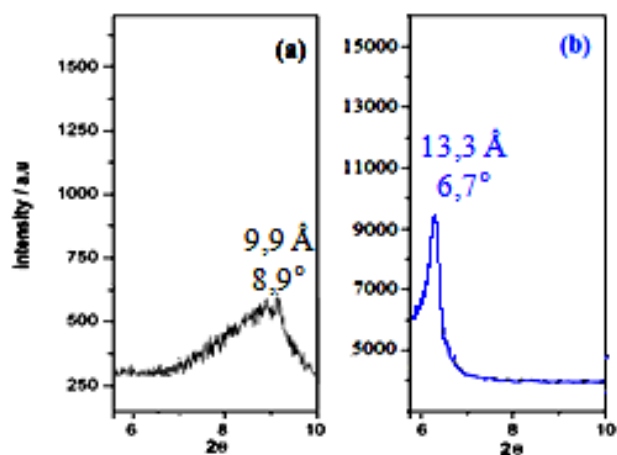


**Figure 8:** XRD patterns of (a) Maghnite-H<sup>+</sup> and (b) MOF-5/Mag-H<sup>+</sup> (25% w).

### 3.3. Thermal properties of MOF-5/Mag-H<sup>+</sup>

The thermal stability of MOF-5 and MOF-5/Mag-H<sup>+</sup> prepared by in situ polymerization process is studied by TGA. The thermograms of MOF-5/Mag-H<sup>+</sup> record a first weight loss at 100°C caused by the removal of water and also a second weight loss from 160°C which is the result of the removal of DMF. MOF-5/Mag-H<sup>+</sup> with different weight percentages of Maghnite-H<sup>+</sup> show high thermal stability up to 465°C for MOF-5 containing 5%wt of Maghnite-H<sup>+</sup> and up to 478°C for MOF-5 containing 50%wt, while that of pure MOF-5 is about 440°C. Thermal stability increases proportionally with the increasing the amount of the clay (Figure 9), a gain of 40°C which is reached at 50%wt of Maghnite-H<sup>+</sup>. This stability is mainly due to the fine dispersion of exfoliated and intercalated particles of Maghnite-H<sup>+</sup> playing an inorganic support for MOF-5.

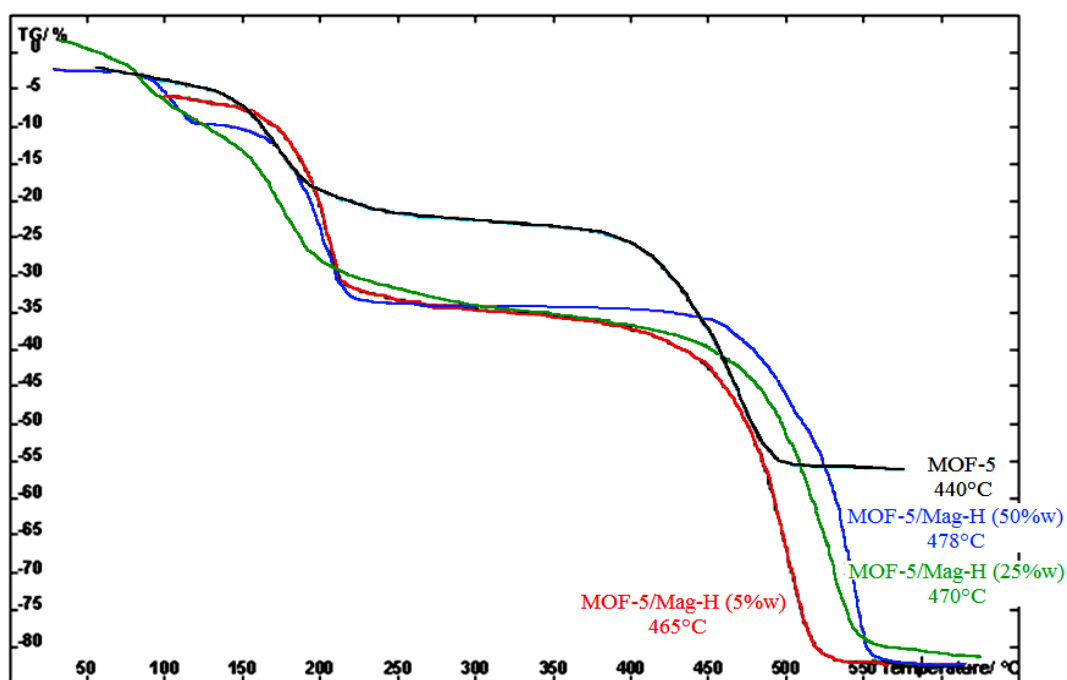


**Figure 9:** Thermograms of MOF-5 and MOF-5/Mag-H<sup>+</sup> (05% w, 25% w, 50% w).

## Conclusions

The objective of this work is to develop an efficient method that respects the principle of green chemistry, using a clay activated by sulfuric acid  $H_2SO_4$  (Maghnite- $H^+$ ) in the synthesis of new hybrid material : MOF-5/Mag- $H^+$ . The spectra of  $^{13}C$  MAS NMR and FTIR confirm the structure of resulting products by showing that there is a complete deprotonation of benzenedicarboxylic acid and then the construction of Zn-O-C group.  $^{27}Al$  and  $^{29}Si$  MAS NMR spectra show that during the in situ polymerization of MOF-5/Mag- $H^+$ , the grafting of the polymer onto the layered silicates is achieved on specific tetracoordinated Al sites without significant chemical change on the aluminosilicate layers of the clay. This conclusion is supported by FRX which shows that Maghnite- $H^+$  used in the synthesis of MOF-5 keeps the same chemical composition in different percentages. Moreover, XRD patterns show that exfoliated/intercalated structures are obtained. The thermal stability of the resulted MOF-5/Mag- $H^+$  is much higher than pure MOF-5. The synthesis of MOF-5 using Maghnite- $H^+$  is very efficient and led to polymerizations with higher yields and better thermal stability which will allow its use in optimal conditions i.e. a degradation temperature which exceeds  $450^\circ C$  without deterioration of the product structure.

**Acknowledgments-** The authors would like to especially thank A. Addou and M. Akeb (Laboratory of Polymer Chemistry, University of Oran, Algeria) for the ATG and FT-IR analysis of polymers. We also appreciate the help of Dr. Violeta Uricanu (PANalytical Application lab. Almelo, The Netherlands) for recording the XRD and FRX analysis.

## References

1. Tranchemontagne D. J., Mendoza-Cortés J. L., O’Keeffe M., Yaghi O., *Chem. Soc. Rev.* 38 (2009) 1257.
2. Kupplera R. J., Timmons D. J., Fanga Q., Lia J., Makala T. A., Younga M. D., Yuana D., Zhaoa D., Zhuanga W., Zhou H., *Coord. Chem. Rev.* 253 (2009) 3042.
3. Wang X., Ma S., Rauch K., Simmons S. M., Yuan D., Wang X., Yildirim T., Cole C. W., Lopez J. J., De Meijere A., Zhou H., *Chem. Mater.* 20 (2008) 3145.
4. Wu H., Zhou W., Yildirim T., *J. Am. Chem. Soc.* 131 (2009) 4995.
5. Dietzel P. D. C., Besikiotis V., Blom R., *J. Mater. Chem.* 19 (2009) 7362.
6. Jung D. W., Yang D. A., Kim J., Ahn W. S., *Dalton Trans.* 39 (2010) 2883.
7. Blanita G., Ardelean O., Lupu D., Borodi G., Mihet M., Coros M., Vlassa M., Misan I., Coldea I., Popeneciu G., *Rev. Roum. Chim.* 56 (2011) 583.
8. Ma M., Zacher D., Zhang X. N., Fischer R. A., Metzler-Nolte N., *Cryst. Growth Des.* 11 (2011) 185.
9. Liu Y. Y., Ng Z. F., Khan E. A., Jeong H. K., Ching C. B., Lai Z. P., *Micropor. Mesopor. Mat.* 118 (2009) 296.
10. Li J. P., Cheng S. J., Zhao Q., Long P. P., Dong J. X., *Int. J. Hydrogen Energy* 34 (2009) 1377.
11. Crawford D., Casaban J., Haydon R., Giri N., McNally T., James S. L., *Chem. Sci.* 6 (2015) 1645.
12. McKinstry C., Cathcart R. J., Cussen E. J., Fletcher A. J., Patwardhan S. V., Sefcik J., *Chem. Eng. J.* 285 (2016) 718.
13. Kaye S. S., Dailly A., Yaghi O. M., Long J. R., *J. Am. Chem. Soc.* 129 (2007) 14176.
14. Chen B., Wang X., Zhang Q., Xi X., Cai J., Qi H., Shi S., Wang J., Yuan D., Fang M., *J. Mater. Chem.* 20 (2010) 3758.
15. Belbachir M., *U.S. Patent.* (2001) 066969.0101.
16. Belbachir M., Bensaoula A., *U.S. Patent.* (2001) US6274527.
17. Eddaoui M., Kim J., Rosi N., Vodak D., Wachter J., O’Keeffe M., Yaghi O. M., *Science* 295 (2002) 469.
18. Komarneni S., Fyfe C. A., Kennedy G. J., Strobl H., *J. Am. Ceram. Soc.* 69 (1986) C45.
19. Ferrahi M. I., Belbachir M., *Int. J. Mol. Sci.* 4 (2003) 312.
20. Harrane A., Meghabar R., Belbachir M., *Des. Monomers Polym.* 8 (2005) 11.
21. Yahiaoui A., Belbachir M., Hachemaoui A., *Int. J. Mol. Sci.* 4 (2003) 548.
22. Yahiaoui A., Belbachir M., Hachemaoui A., *Int. J. Mol. Sci.* 4 (2003) 572.
23. Breen C., Madejová J., Komadel P., *J. Mater. Chem.* 3 (1995) 496.
24. Tkáč I., Komadel P., Müller D., *Clay Miner.* 29 (1994) 11.
25. Hafizovic J., Bjorgen M., Olsbye U., Dietzel P. D. C., Bordiga S., Prestipino C., Lamberti C., Lillerud K. P., *J. Am. Chem. Soc.* 129 (2007) 3612.

(2017) ; <http://www.jmaterenvironsci.com>